Relativistic static thin dust disks with an inner edge: An infinite family of new exact solutions

Guillermo A. González,[1,2,*] Antonio C. Gutiérrez-Piñeres,[1,†] and Viviana M. Viña-Cervantes[1,‡]

[1] *Escuela de Física, Universidad Industrial de Santander, A. A. 678, Bucaramanga, Colombia*

[2] *Departamento de Física Teórica, Universidad del País Vasco, 48080 Bilbao, Spain*

(Received 24 November 2008; revised manuscript received 17 May 2009; published 30 June 2009)

An infinite family of new exact solutions of the vacuum Einstein equations is presented. The solutions are static and axially symmetric and correspond to an infinite family of thin dust disks with a central inner edge. The metric functions of all the solutions can be explicitly computed, and can be expressed in a simple manner in terms of oblate spheroidal coordinates. The energy density of all the disks of the family is positive everywhere and well behaved, so that the corresponding energy-momentum tensor is in full agreement with all the energy conditions. Moreover, although the total mass of the disks is infinite, the solutions are asymptotically flat and the Riemann tensor is regular everywhere, as it is shown by computing the curvature scalars. Now, besides its importance as a new family of exact solutions of the vacuum Einstein equations, the main importance of this family of solutions is that it can be easily superposed with the Schwarzschild solution in order to describe thin disks surrounding a central black hole. Accordingly, a detailed analysis of this superposition will be presented in a subsequent paper.

DOI: 10.1103/PhysRevD.79.124048 PACS numbers: 04.20.Jb, 04.40.−b

I. INTRODUCTION

The observational data supporting the existence of black holes at the nucleus of some galaxies is today so abundant, with the strongest dynamical evidence coming from the center of the Milky Way, that there is no doubt about the relevance of the study of binary systems composed by a thin disk surrounding a central black hole (see [1,2] for recent reviews on the observational evidence). Consequently, great deal of work has been developed in the last years in order to obtain a better understanding of the different aspects involved in the dynamics of these systems. Now, due to the presence of a black hole, the gravitational fields involved are so strong that the proper theoretical framework to analytically study these configurations is provided by the general theory of relativity. Therefore, a strong effort has been dedicated to the obtaining of exact solutions of the Einstein equations corresponding to thin disklike sources with a central black hole (see [3,4] for thorough surveys on the subject).

Stationary and axially symmetric solutions of the Einstein vacuum equations are of obvious astrophysical importance, as they describe the exterior of equilibrium configurations of rotating bodies. Specifically, such spacetimes are the best choice to attempt to describe the gravitational fields of disks around black holes in an exact analytical manner. So, through the years, examples of solutions corresponding to black holes or to thin disklike sources have been obtained by several different techniques. However, due to the nonlinear character of the Einstein equations, solutions corresponding to the superposition of black holes and thin disks are not so easy to obtain and therefore, until now, very few exact stationary solutions have been obtained.

On the other hand, if we only consider static configurations, the line element is characterized by two metric functions only. In the vacuum case, the Einstein equations imply that one of the metric functions satisfies the Laplace equation, while the other one can be obtained by quadratures. Furthermore, since the sources are infinitesimally thin disks, the matter only enters in the form of boundary conditions for the vacuum equations. Therefore, as a consequence of the linearity of the Laplace equation, solutions corresponding to the superposition of thin disks and black holes can be, in principle, easily obtained.

However, if we consider thin disks that extend up to the event horizon, the matter located near the black hole would move with superluminal velocities, as it was shown by Lemos and Letelier [5–7]. So, in order to prevent the appearance of tachyonic matter, the thin disks must have an inner edge with a radius larger than the photonic radius of the black hole. Hence, the boundary value problem for the Laplace equation is mathematically more complicated and thus only very few exact solutions have been obtained. Solutions of this kind were first studied by Lemos and Letelier [6] by making a Kelvin transformation in order to invert the Morgan and Morgan [8] family of finite thin disks. Now, although the second metric function of this solution cannot be analytically obtained, its main properties were extensively analyzed in a series of papers by Semerák, Žáček, and Zellerin [9–15], by using numerical computation when was needed.

It is then clear that the obtaining of exact solutions that properly describe thin disklike sources with an inner edge has a manifest relevance in the study of binary systems that involve a central black hole. Indeed, as it was pointed out in

*guillego@uis.edu.co
†agutierrez@ciencias.uis.edu.co
‡vivo1225@gmail.com

[16], the main properties of these annular disks strongly depend on their specific density profiles. Therefore, it is worth having other solutions, in addition to those obtained previously, in such a way that a detailed study of such systems can be made. Furthermore, with explicitly integrated solutions the analytical study of the geodesics can be easily performed, allowing one to attain a clear understanding of their main dynamical aspects. Also, the static solutions can be considered as the first step toward the obtaining of the most realistic stationary solutions, which can be obtained from the previous ones by means of well-known methods of solution generation.

Now, apart from the Lemos and Letelier inverted disks, only two other solutions for static thin disks with an inner edge have been obtained, one with inverted isochrone disks [17] and another for disks with a power-law density [16]. Also, a stationary superposition was obtained by Zellerin and Semerák [18] by using the Belinskii-Zakahrov inverse-scattering method, but the analysis of its properties is complicated by the fact that the metric functions cannot be analytically computed. Furthermore, this solution involves an unphysical supporting surface between the black hole horizon and the disk [19]. Finally, a general class of stationary solutions was presented by Klein [20], by using the Riemann-surface techniques, with which physically acceptable black hole disk systems can in principle be found (see also [21]).

In agreement with the above considerations, in this paper we present an infinite family of new exact solutions for static thin dust disks with a central inner edge. In order to find these solutions we will introduce a coordinate system naturally adapted to the geometry of the source, in such a way that the boundary value problem for the Laplace equation can be properly posed. These coordinates also allow one to explicitly compute the metric functions of all the solutions. The solutions thus obtained describe disks whose energy densities are everywhere positive and well behaved, in such a way that their energy-momentum tensors are in full agreement with all the energy conditions. Now, although the total mass of the disks is infinite, the solutions are asymptotically flat and their Riemann tensors are regular everywhere, as it is shown by computing the curvature scalars.

The paper is organized as follows. First, in Sec. II, we present the formulation of the Einstein equations for static axially symmetric spacetimes with an infinitesimally thin disk as a source. We also present the proper boundary conditions and their relationship with the physical quantities characterizing the sources. Then, in Sec. III, we introduce oblate spheroidal coordinates with the ranges chosen in such a way that they are naturally adapted to the geometry of a thin disk with a central inner edge. The Einstein equations are then solved and the metric functions of the whole family of solutions are explicitly computed and the expressions obtained are simply written in terms of the oblate spheroidal coordinates.

The analysis of the physical behavior of the solutions is then presented in Sec. IV, where we analyze first the asymptotic behavior of the solution of the Laplace equation, in order to determine their leading multipolar moments. After that, we study the behavior of the corresponding energy densities and pressures, as well as the corresponding mass densities, relativistic and Newtonian, and we compute the total mass of the disks. Finally, we analyze the behavior of the Riemann curvature tensor by computing its invariants. We conclude, in Sec. V, by summarizing our main results.

II. THE EINSTEIN EQUATIONS WITH THIN DISKLIKE SOURCES

In order to formulate the Einstein equations for static axially symmetric spacetimes with an infinitesimally thin disk as a source, we first introduce coordinates $x^a = (t, \varphi, r, z)$ in which the metric tensor only depends on r and z. We assume that these coordinates are quasicylindrical in the sense that the coordinate r vanishes on the axis of symmetry and, for fixed z, increases monotonically to infinity, while the coordinate z, for fixed r, increases monotonically in the interval $(-\infty, \infty)$. The azimuthal angle φ ranges in the interval $[0, 2\pi)$, as usual [22]. We also assume that there exists an infinitesimally thin disk, located at the hypersurface $z = 0$, so that the components of the metric tensor are symmetrical functions of z and their first z derivatives have a finite discontinuity at $z = 0$.

With the above considerations, we have

$$g_{ab}(r, -z) = g_{ab}(r, z), \tag{1}$$

so that, for $z \neq 0$,

$$g_{ab,z}(r, -z) = -g_{ab,z}(r, z). \tag{2}$$

Hence, the metric tensor is continuous at $z = 0$,

$$[g_{ab}] = g_{ab}|_{z=0^+} - g_{ab}|_{z=0^-} = 0, \tag{3}$$

while the discontinuities in the derivatives of the metric tensor can be written as

$$\gamma_{ab} = [g_{ab,z}] = 2g_{ab,z}|_{z=0^+}, \tag{4}$$

where the reflection symmetry with respect to $z = 0$ has been used. Therefore, using the distributional approach [23–25] (or the junction conditions on the extrinsic curvature of thin shells [26–28]), we can write the metric tensor as

$$g_{ab} = g^+_{ab}\theta(z) + g^-_{ab}\{1 - \theta(z)\}, \tag{5}$$

and thus the Ricci tensor reads

$$R_{ab} = R^+_{ab}\theta(z) + R^-_{ab}\{1 - \theta(z)\} + H_{ab}\delta(z), \tag{6}$$

where $\theta(z)$ and $\delta(z)$ are, respectively, the Heaveside and Dirac distributions with support on $z = 0$. Here $g^\pm_{ab}$ and $R^\pm_{ab}$ are the metric tensors and the Ricci tensors of the $z \geq$

0 and $z \leq 0$ regions, respectively, and

$$H_{ab} = \frac{1}{2}\{\gamma^z_a \delta^z_b + \gamma^z_b \delta^z_a - \gamma^c_c \delta^z_a \delta^z_b - g^{zz}\gamma_{ab}\}, \quad (7)$$

where all the quantities are evaluated at $z = 0^+$.

In agreement with (6), the energy-momentum tensor must be expressed as

$$T_{ab} = T^+_{ab}\theta(z) + T^-_{ab}\{1 - \theta(z)\} + Q_{ab}\delta(z), \quad (8)$$

where $T^\pm_{ab}$ are the energy-momentum tensors of the $z \geq 0$ and $z \leq 0$ regions, respectively, and Q_{ab} gives the part of the energy-momentum tensor corresponding to the disklike source. The "true" surface energy-momentum tensor of the disk S_{ab} can be obtained through the relation

$$S_{ab} = \int Q_{ab}\delta(z)ds_n = \sqrt{g_{zz}}Q_{ab}, \quad (9)$$

where $ds_n = \sqrt{g_{zz}}dz$ is the "physical measure" of length in the direction normal to the $z = 0$ plane.

Accordingly, the Einstein equations, in geometrized units such that $c = 8\pi G = 1$, are equivalent to the system of equations

$$R^\pm_{ab} - \frac{1}{2}g_{ab}R^\pm = T^\pm_{ab}, \quad (10)$$

with the boundary conditions

$$H_{ab} - \frac{1}{2}g_{ab}H = Q_{ab}, \quad (11)$$

where $H = g^{ab}H_{ab}$ and, again, all the quantities are evaluated at $z = 0^+$. When the thin disk is the only source of the gravitational field, i.e. $T^\pm_{ab} = 0$, Eq. (10) reduces to the Einstein vacuum equations

$$R^\pm_{ab} = 0, \quad (12)$$

for the $z \geq 0$ and $z \leq 0$ regions, respectively. Thus, in order to obtain solutions with a thin disk as source, we must solve the system (12) using the boundary conditions (11) with the values of Q_{ab} that describe properly the matter content of the disk.

Now, in order to obtain explicit forms for the vacuum Einstein equations and the boundary conditions, we will take the metric tensor as given by the Weyl line element, which reads [29]

$$ds^2 = -e^{2\Phi}dt^2 + e^{-2\Phi}[r^2d\varphi^2 + e^{2\Lambda}(dr^2 + dz^2)], \quad (13)$$

where Φ and Λ are continuous functions of r and z. Furthermore, we will assume that Φ and Λ are even functions of z,

$$\Phi(r, -z) = \Phi(r, z), \quad (14a)$$

$$\Lambda(r, -z) = \Lambda(r, z), \quad (14b)$$

so that their first z derivatives are odd functions of z,

$$\Phi_{,z}(r, -z) = -\Phi_{,z}(r, z), \quad (15a)$$

$$\Lambda_{,z}(r, -z) = -\Lambda_{,z}(r, z), \quad (15b)$$

which we shall require that do not vanish at $z = 0$.

With the previous assumptions, the vacuum Einstein equations (12) reduce to the system

$$(r\Phi_{,r})_{,r} + (r\Phi_{,z})_{,z} = 0, \quad (16a)$$

$$\Lambda_{,r} = r(\Phi^2_{,r} - \Phi^2_{,z}), \quad (16b)$$

$$\Lambda_{,z} = 2r\Phi_{,r}\Phi_{,z}, \quad (16c)$$

where (16a) is the usual Laplace equation for an axially symmetric source in cylindrical coordinates. The integrability condition for the overdetermined system (16b) and (16c) is granted when Φ is a solution of (16a), and thus Λ can be obtained by quadratures given a solution Φ. On the other hand, Eq. (11) yields the boundary conditions

$$2e^{2(\Phi-\Lambda)}[\Lambda_{,z} - 2\Phi_{,z}] = Q^t_t, \quad (17a)$$

$$2e^{2(\Phi-\Lambda)}\Lambda_{,z} = Q^\varphi_\varphi, \quad (17b)$$

where all the quantities are evaluated at $z = 0^+$.

In agreement with the above expressions, the consistency of the Einstein equations implies that S_{ab} must have only two nonzero components. So, by using the orthonormal tetrad

$$V^a = e^{-\Phi}\delta^a_t, \quad (18a)$$

$$W^a = e^{\Phi}\delta^a_\varphi/r, \quad (18b)$$

$$X^a = e^{\Phi-\Lambda}\delta^a_r, \quad (18c)$$

$$Y^a = e^{\Phi-\Lambda}\delta^a_z, \quad (18d)$$

we can write the surface energy-momentum tensor S_{ab} in the canonical form

$$S_{ab} = \epsilon V_a V_b + pW_a W_b, \quad (19)$$

where ϵ and p are, respectively, the energy density and the azimuthal pressure of the disk. Now, using (19), it is easy to see that the surface mass density of the disk reduces to

$$\mu = \epsilon + p, \quad (20)$$

where μ has been defined as

$$\mu = 2\left(S_{ab} - \frac{1}{2}g_{ab}S\right)V^aV^b, \quad (21)$$

with $S = g^{ab}S_{ab}$ and, as before, the expression is evaluated at $z = 0^+$.

The energy-momentum tensor can also be interpreted as the superposition of two counterrotating fluids that circulate in opposite directions. In order to do this, we cast S^{ab} as [30]

$$S^{ab} = \epsilon_+ V^a_+ V^b_+ + \epsilon_- V^a_- V^b_-, \quad (22)$$

where

$$\epsilon_+ = \epsilon_- = \frac{\epsilon - p}{2}, \tag{23}$$

are the energy densities of the two counterrotating fluids, and we take the two fluids moving along geodesics with equal but opposite velocities. So, the velocity vectors of the two counterrotating fluids are given by [30]

$$V_\pm^a = \frac{V^a \pm UW^a}{\sqrt{1-U^2}}, \tag{24}$$

where

$$U^2 = \frac{p}{\epsilon}, \tag{25}$$

is the counterrotating tangential velocity.

As we can see from the expressions above, the most general energy-momentum tensor compatible with the line element (13) and the boundary conditions (11) corresponds to a thin disklike source that has only nonzero energy density and azimuthal pressure. In agreement with this, instead of giving specific prescriptions for the energy density and the azimuthal pressure, the Einstein equations will be solved by requiring only that these two quantities are different from zero at the surface of a disk with an inner edge. Then, after a given solution will be obtained, it can be used in order to obtain, from the boundary conditions, the corresponding expressions for the energy density and the azimuthal pressure. Therefore, the solution will correspond to the most general static thin disk with an inner edge that can be obtained by exactly solving the Einstein equations.

Now, in terms of the energy density and the azimuthal pressure, the boundary conditions read

$$2e^{\Phi-\Lambda}[2\Phi_{,z} - \Lambda_{,z}] = \epsilon, \tag{26a}$$

$$2e^{\Phi-\Lambda}\Lambda_{,z} = p. \tag{26b}$$

So, by using (16c), we can cast these conditions as

$$4e^{\Phi-\Lambda}[1 - r\Phi_{,r}]\Phi_{,z} = \epsilon, \tag{27a}$$

$$4e^{\Phi-\Lambda}r\Phi_{,r}\Phi_{,z} = p. \tag{27b}$$

Also, thanks to (20), we have that

$$4e^{\Phi-\Lambda}\Phi_{,z} = \mu, \tag{28}$$

where, as before, all the quantities are evaluated at $z = 0^+$. Accordingly, in order to obtain a solution representing a thin disk located at the hypersurface $z = 0$, with a circular central inner edge of radius a, we only need to impose that

$$\Phi_{,z}(r, 0^+) = \begin{cases} 0; & 0 \le r \le a, \\ f(r); & r \ge a, \end{cases} \tag{29}$$

with $f(r)$ being an arbitrary function. Then, only after we find the most general solution, we will impose additional conditions in order to have a physically reasonable behavior.

In agreement with the above considerations, in order to have an asymptotically flat spacetime, we will require that

$$\lim_{R\to\infty} \Phi(r, z) = 0, \tag{30a}$$

$$\lim_{R\to\infty} \Lambda(r, z) = 0, \tag{30b}$$

where $R^2 = r^2 + z^2$. Also, in order to have regularity at the symmetry axis, we will require that

$$\Phi(0, z) < \infty, \tag{31a}$$

$$\Lambda(0, z) = 0. \tag{31b}$$

We will also require that

$$f(r) \ge 0, \tag{32a}$$

$$0 \le r\Phi_{,r} \le 1, \tag{32b}$$

in order that the mass density, the energy density and the azimuthal pressure be positive everywhere.

On the other hand, from (23) and (25), we can see that the energy densities of the two counterrotating fluids can be written as

$$\epsilon_\pm = 2e^{\Phi-\Lambda}[1 - 2r\Phi_{,r}]\Phi_{,z}, \tag{33}$$

while the counterrotating tangential velocity is given by

$$U^2 = \frac{r\Phi_{,r}}{1 - r\Phi_{,r}}. \tag{34}$$

Consequently, in order to have a well behaved counterrotating model, we need to impose a stronger condition than (32b). So, instead, we will require that

$$0 \le 2r\Phi_{,r} \le 1, \tag{35}$$

in order that the energy density of the two counterrotating fluids be positive everywhere, $\epsilon_\pm \ge 0$, and that the counterrotating tangential velocity be real and less than the velocity of light, $0 \le U^2 \le 1$.

III. SOLUTION OF THE EINSTEIN EQUATIONS

In order to solve the Einstein vacuum equations, we must first solve the boundary value problem for Φ. However, due to the nature of the boundary conditions (29), it is convenient to look for a different coordinate system naturally adapted to the geometry of the source. Accordingly, we introduce the oblate spheroidal coordinates, defined through the relations

$$r^2 = a^2(1 + x^2)(1 - y^2), \tag{36a}$$

$$z = axy, \tag{36b}$$

so that

$$x^2 = \frac{\sqrt{(r^2 + z^2 - a^2)^2 + 4a^2z^2} + (r^2 + z^2 - a^2)}{2a^2}, \tag{37a}$$

$$y^2 = \frac{\sqrt{(r^2 + z^2 - a^2)^2 + 4a^2z^2} - (r^2 + z^2 - a^2)}{2a^2}. \tag{37b}$$

This transformation involves a one-to-four correspondence of points in the (r, z) plane to points in the (x, y) plane. Hence, in order to have a one-to-one correspondence that spans the entire (r, z) plane, we must properly restrict the ranges of the oblate spheroidal coordinates (x, y).

There are four possible choices of the ranges of the (x, y) that lead to a one-to-one correspondence. We can take, as it is commonly done, $0 \leq x < \infty$ and $-1 \leq y \leq 1$, so that the interval $0 \leq r \leq a$ with $z = 0^+$ is mapped into the interval $x = 0$, $0 \leq y \leq 1$, whereas the interval $0 \leq r \leq a$ with $z = 0^-$ is mapped into the interval $x = 0$, $-1 \leq y \leq 0$. That is, we have a cut line at the interval $0 \leq r \leq a$. Accordingly, since y changes sign on crossing this cut line, but does not change in absolute value, this coordinate has a finite discontinuity when $x = 0$, while the coordinate x is continuous everywhere. Hence, an even function of y is continuous everywhere but has a discontinuous normal derivative at $x = 0$. The same behavior occurs if, instead, the range of x is taken to be $-\infty < x \leq 0$. Therefore, either one of these two choices of the ranges must be used to describe a finite thin disk of radius $r = a$ located at $z = 0$.

On the other hand, a different behavior can be obtained if we take the ranges to be $-\infty < x < \infty$ and $0 \leq y \leq 1$. In this case the interval $a \leq r < \infty$ with $z = 0^+$ is mapped into the interval $y = 0$, $0 \leq x < \infty$, whereas the interval $a \leq r < \infty$ with $z = 0^-$ is mapped into the interval $y = 0$, $-\infty < x \leq 0$. Then, the cut line will be at the interval $a \leq r < \infty$. So, since x changes sign on crossing the cut line, but does not change in absolute value, this coordinate has a finite discontinuity when $y = 0$, while the coordinate y is continuous everywhere. Therefore, an even function of x is continuous everywhere but has a discontinuous normal derivative at $y = 0$. The same behavior occurs if we take the range of y to be $-1 \leq y \leq 0$. Accordingly, these two choices of ranges are indicated in order to describe an infinite disklike source, with a circular central inner edge of radius a, located at $z = 0$.

As a consequence, we will take the ranges of (x, y) to be $-\infty < x < \infty$ and $0 \leq y \leq 1$. So, when $x = 0$ we have $z = 0$ and $0 \leq r \leq a$, whereas when $y = 0$ we have $z = 0$ and $r \geq a$. That is, the surface $y = 0$ describes a thin disk with an inner edge of radius a, while the surface $x = 0$ describes the vacuum hole inside this edge. On the other hand, the z axis is described by $y = 1$ since, in this case, we have $r = 0$ and $-\infty < z < \infty$. Then, in order that $\Phi(x, y)$ be continuous everywhere, we will take it to be an even function of x

$$\Phi(-x, y) = \Phi(x, y), \tag{38}$$

so that

$$\Phi_{,x}(-x, y) = -\Phi_{,x}(x, y), \tag{39}$$

and thus conditions (14a) and (15a) are trivially satisfied.

In the oblate spheroidal coordinates, the Weyl line element (13) can be rewritten as

$$ds^2 = -e^{2\Phi}dt^2 + a^2(1 + x^2)(1 - y^2)e^{-2\Phi}d\varphi^2 + a^2(x^2 + y^2)e^{2(\Lambda-\Phi)}\left[\frac{dx^2}{1 + x^2} + \frac{dy^2}{1 - y^2}\right], \tag{40}$$

and the Einstein vacuum equations reduce to

$$[(1 + x^2)\Phi_{,x}]_{,x} + [(1 - y^2)\Phi_{,y}]_{,y} = 0, \tag{41}$$

the Laplace equation in oblate spheroidal coordinates, and the overdetermined system

$$\Lambda_{,x} = (1 - y^2)[x(1 + x^2)\Phi_{,x}^2 - x(1 - y^2)\Phi_{,y}^2 - 2y(1 + x^2)\Phi_{,x}\Phi_{,y}]/(x^2 + y^2), \tag{42a}$$

$$\Lambda_{,y} = (1 + x^2)[y(1 + x^2)\Phi_{,x}^2 - y(1 - y^2)\Phi_{,y}^2 + 2x(1 - y^2)\Phi_{,x}\Phi_{,y}]/(x^2 + y^2), \tag{42b}$$

whose integrability condition is granted by Eq. (41).

On the other hand, by using (36a) and (36b), it is easy to see that

$$\Phi_{,z}(r, 0) = \begin{cases} \Phi_{,x}(0, y)/ay; & 0 \leq r \leq a, \\ \Phi_{,y}(x, 0)/ax; & r \geq a. \end{cases} \tag{43}$$

Accordingly, due to the reflection symmetry of the solutions, the conditions (29) are equivalent to

$$\Phi_{,x}(0, y) = 0, \tag{44a}$$

$$\Phi_{,y}(x, 0) = F(x), \tag{44b}$$

with $F(x)$ being an arbitrary even function of x. The general solution of Eq. (41) with these boundary conditions is given by [31]

$$\Phi(x, y) = \sum_{n=0}^{\infty}[A_{2n}P_{2n}(y) + B_{2n}Q_{2n}(y)]p_{2n}(x), \tag{45}$$

where A_{2n} and B_{2n} are constants, $P_{2n}(y)$ and $Q_{2n}(y)$ are the Legendre polynomials and the Legendre functions of the second kind, respectively, and $p_{2n}(x) = i^{-2n}P_{2n}(ix)$. Therefore, all the solutions of the Einstein vacuum equations for static spacetimes, with any axially symmetric source such as the one considered here, are obtained by taking for the metric function $\Phi(x, y)$ any particular choice of the above general solution, or expressions obtained from these solutions by means of linear operations.

Now, in terms of the oblate spheroidal coordinates, condition (30a) is written as

$$\lim_{x\to\infty}\Phi(x, y) = 0, \tag{46}$$

whereas condition (31a) reads

$$\Phi(x, 1) < \infty. \tag{47}$$

Therefore, due to the behavior of the Legendre functions, it is clear that it is not possible to fulfill these conditions with any particular choice of the general solution (45). However, by considering only the first term of the series,

$$\Phi_0(x, y) = A_0 + B_0 Q_0(y), \tag{48}$$

we obtain a solution that is regular for all $y \neq 1$. Then, if we take $A_0 = 0$, this solution can be written as

$$\Phi_0(x, y) = \frac{\alpha}{2} \ln\left[\frac{1+y}{1-y}\right], \tag{49}$$

where α is an arbitrary constant, so that a direct integration of (42a) and (42b) gives

$$\Lambda_0(x, y) = \frac{\alpha^2}{2} \ln\left[\frac{1-y^2}{x^2+y^2}\right], \tag{50}$$

where the integration constant has been taken to be zero. We can easily check that this solution is not asymptotically flat nor regular at the symmetry axis. Nevertheless, by using (26a) and (26b), we obtain for the energy density and the azimuthal pressure the expressions

$$\epsilon = (4\alpha/a)x^{\alpha^2-1}, \tag{51a}$$

$$p = 0, \tag{51b}$$

and thus, if $\alpha > 0$, the disk satisfies all the energy conditions [32]. However, for any value of $\alpha \neq 1$, the energy density increases without limit, either at infinity or at the inner edge of the disk. Alternatively, for $\alpha = 1$ the energy density is everywhere constant. Therefore, in any case, the total mass of the disk will be infinite.

On the other hand, although the previous solution has not a physically acceptable behavior, we can use it as the starting point to generate new solutions with a better behavior. In order to do this, we consider the oblate spheroidal coordinates not only as functions of the cylindrical coordinates (r, z), but also parametrically dependent on the radius a,

$$x = x(r, z; a), \tag{52a}$$

$$y = y(r, z; a). \tag{52b}$$

Then, by considering also the metric function Φ dependent on a,

$$\Phi = \Phi(r, z; a), \tag{53}$$

we can obtain a family of new solutions by applying the linear operation

$$\Phi_{n+1}(r, z; a) = \frac{\partial \Phi_n(r, z; a)}{\partial a}, \tag{54}$$

where n is an integer, $n \geq 0$.

Thus, by starting with the "seed" solution $\Phi_0(x, y)$, by means of the previous procedure one generates a family of new solutions that can be written in the simple form

$$\Phi_n(r, z; a) = \Phi_n(x, y) = \frac{\alpha y F_n(x, y)}{a^n (x^2 + y^2)^{2n-1}}, \tag{55}$$

for $n \geq 1$, where the $F_n(x, y)$ are polynomial functions, with highest degree $4n - 4$, of which we present below the first three only,

$$F_1 = 1,$$

$$F_2 = x^4 + 3x^2(1 - y^2) - y^2,$$

$$\begin{aligned} F_3 = {} & 3x^6(3 - 5y^2) + 5x^4(6y^4 - 11y^2 + 3) \\ & - x^2y^2(3y^4 - 31y^2 + 30) - y^4(y^2 - 3). \end{aligned}$$

The rest can be easily obtained by means of (54). It is easy to see that

$$\lim_{x\to\infty} \Phi_n(x, y) = 0, \tag{56a}$$

$$\Phi_n(x, 1) < \infty, \tag{56b}$$

in full agreement with conditions (30a) and (31a).

Now, in order to obtain the corresponding metric functions $\Lambda_n(r, z; a)$, we integrate

$$\Lambda_n(r, z; a) = \Lambda_n(x, y) = \int_1^y \Lambda_{,y}(x, y) dy, \tag{57}$$

by taking $\Lambda_n(x, 1) = 0$ in order to grant regularity at the axis. So, by using (55) in (42b), the solutions obtained can be written in the simple form

$$\Lambda_n(x, y) = \frac{\alpha^2 (2n-2)!(y^2 - 1)A_n(x, y)}{4^n a^{2n} (x^2 + y^2)^{4n}}, \tag{58}$$

for $n \geq 1$, where the $A_n(x, y)$ are polynomial functions, of highest degree $8n - 2$, of which we present here the first three only,

$$A_1 = x^4(9y^2 - 1) + 2x^2y^2(y^2 + 3) + y^4(y^2 - 1),$$

$$\begin{aligned} A_2 = {} & 2x^{12}(9y^2 - 1) - 4x^{10}(51y^4 - 41y^2 + 2) \\ & + x^8(735y^6 - 1241y^4 + 419y^2 - 9) \\ & - x^6y^2(132y^6 - 1644y^4 + 1604y^2 - 252) \\ & + x^4y^4(84y^6 - 384y^4 + 1266y^2 - 630) \\ & + 4x^2y^6(6y^6 + 6y^4 - 39y^2 + 63) \\ & + 3y^8(y^6 + y^4 + y^2 - 3), \end{aligned}$$

$$A_3 = 3x^{16}(1225y^6 - 1275y^4 + 315y^2 - 9) - 24x^{14}(980y^8 - 2095y^6 + 1205y^4 - 189y^2 + 3) + 2x^{12}(24\,255y^{10} - 89\,475y^8 + 98\,472y^6 - 36\,316y^4 + 3473y^2 - 25) - 12x^{10}y^2(1835y^{10} - 16\,665y^8 + 34\,716y^6 - 25\,292y^4 + 6001y^2 - 275) + 6x^8y^4(900y^{10} - 11\,946y^8 + 50\,563y^6 - 69\,397y^4 + 33\,365y^2 - 4125) + 8x^6y^6(125y^{10} + 926y^8 - 9079y^6 + 24\,639y^4 - 22\,290y^2 + 5775) + 6x^4y^8(55y^{10} + 29y^8 + 764y^6 - 4808y^4 + 8469y^2 - 4125) + 12x^2y^{10}(5y^{10} + 5y^8 + 80y^4 - 301y^2 + 275) + y^{12}(5y^{10} + 5y^8 + 5y^6 + y^4 + 34y^2 - 50).$$

The rest can be obtained as the result of computing the integral (57). We can easily check that

$$\lim_{x\to\infty} \Lambda_n(x, y) = 0, \tag{59a}$$

$$\Lambda_n(x, 1) = 0, \tag{59b}$$

in full agreement with conditions (30b) and (31b).

IV. BEHAVIOR OF THE SOLUTIONS

In order to analyze the physical behavior of the previously obtained family of solutions, in the first instance we will consider the behavior of $\Phi_n(r, z; a)$ for large values of R, where $R^2 = r^2 + z^2$. From (36a) and (36b) it is easy to see that, when $R \to \infty$, the spheroidal coordinates (x, y) behave as

$$x \sim R/a, \tag{60a}$$

$$y \sim z/R. \tag{60b}$$

Then, from the expressions for $F_n(x, y)$, it is easy to check that

$$F_n \sim \begin{cases} x^{3n-3}; & n = 1, 3, \ldots, \\ x^{3n-2}; & n = 2, 4, \ldots, \end{cases} \tag{61}$$

so that

$$\Phi_n \sim \begin{cases} z/R^{n+2}; & n = 1, 3, \ldots, \\ z/R^{n+1}; & n = 2, 4, \ldots. \end{cases} \tag{62}$$

Consequently, Φ_1 and Φ_2 behave as dipoles, Φ_3 and Φ_4 as quadrupoles, Φ_5 and Φ_6 as octopoles, and so on. However, although there is no monopole term in Φ_n, the total mass of the source is not zero, as we will show below.

In order to analyze the behavior of the corresponding disklike sources, we will first compute their azimuthal pressure. From (36a) and (36b) it follows that

$$\Phi_{,r}(r, 0) = \left[\frac{\sqrt{1 + x^2}}{ax}\right]\Phi_{,x}(x, 0), \qquad r \geq a, \tag{63}$$

and, by using (55), it is easy to prove that

$$\Phi_{n,x}(x, 0) = 0. \tag{64}$$

Then, (27b) yields

$$p_n = 0. \tag{65}$$

That is, all the disks of the family have zero azimuthal pressure. Furthermore, from (25) we can see that all the disks have zero counterrotating tangential velocity,

$$U = 0. \tag{66}$$

Therefore, these disks can be considered as "truly static disks" in the sense that we cannot obtain a counterrotating interpretation for them.

On the other hand, by using Eqs. (20), (28), (55), and (58), the surface energy density of the disks can be calculated to give

$$\epsilon_n(x) = \frac{4\alpha E_n(x)}{a^{n+1}x^{2n+1}} \exp\left\{-\frac{\alpha^2(2n-2)!B_n(x)}{2^{2n}a^{2n}x^{4n}}\right\}, \tag{67}$$

where $x \geq 0$. In this expression, the $E_n(x)$ are positive definite polynomials of degree $2k$, with $k = (n-1)/2$ for odd n and $k = n/2$ for even n, of which we will write below the first three only,

$$E_1(x) = 1,$$

$$E_2(x) = x^2 + 3,$$

$$E_3(x) = 3(x^2 + 5),$$

all of them, as well of the rest, easily computed from (55). The $B_n(x)$ are positive definite polynomials of degree $4k$, with $k = (n-1)/2$ for odd n and $k = n/2$ for even n, the first three of them given by

$$B_1(x) = 1,$$

$$B_2(x) = 2x^4 + 8x^2 + 9,$$

$$B_3(x) = 27x^4 + 72x^2 + 50,$$

all of them, as well of the rest, easily computed from (58).

From the above expressions we can see that, by taking $\alpha > 0$, the energy density of the disks will be everywhere positive,

$$\epsilon_n(x) \geq 0. \tag{68}$$

Therefore, since the azimuthal pressure is zero, we have an infinite family of dust disks that satisfy all the energy conditions. It is also easy to see that, for any value of n,

$$\epsilon_n(0) = 0, \tag{69a}$$

$$\lim_{x\to\infty} \epsilon_n(x) = 0. \tag{69b}$$

That is, the energy density of the disks is zero at their inner edge and vanishes at infinite. Moreover, since the azimuthal pressure is zero, the surface mass density of the disks reduces to their energy density,

$$\mu_n(x) = \epsilon_n(x), \tag{70}$$

and therefore, its behavior is the same as that of the energy density.

Now, in order to show the behavior of the energy densities, we plot the dimensionless surface energy densities $\tilde{\epsilon}_n = a\epsilon_n$ as functions of the dimensionless radial coordinate $\tilde{r} = r/a$. So, in Fig. 1, we plot $\tilde{\epsilon}_n$ as a function of $\tilde{r}$ for the first three disks of the family, with $n = 1$, 2, and 3, for different values of the parameter $\tilde{\alpha}_n = \alpha/a^n$. Then, for each value of n, we take $\tilde{\alpha}_n = 0.5$, 1, 1.5, 2, 2.5, 3, 3.5, and 4. The first curve on the left corresponds to $\tilde{\alpha}_n = 0.5$, while the last curve on the right corresponds to $\tilde{\alpha}_n = 4$. As we can see, in all the cases the surface energy density is positive everywhere, having a maximum near the inner edge of the disks, and then rapidly decreasing as $\tilde{r}$ increases. We can also see that, for a fixed value of n, as the value of $\tilde{\alpha}_n$ increases, the value of the maximum diminishes and moves toward increasing values of $\tilde{r}$. The same behavior is observed for a fixed value of $\tilde{\alpha}_n$ and increasing values of n.

Furthermore, since the gravitational potential in Newtonian theory is given by the solution of the boundary value problem for the Laplace equation, we can consider the $\Phi_n(r, z; a)$ as a family of Newtonian gravitational potentials of thin disklike sources with an inner edge, whose Newtonian mass densities are given by

$$\sigma_n(x) = 4\Phi_{n,z}|_{z=0^+} = \frac{4\alpha E_n(x)}{a^{n+1}x^{2n+1}}, \tag{71}$$

clearly diverging at the inner edge of the disks. That is, the behavior of the surface mass densities in the general relativistic disk models is better than in the corresponding Newtonian models. On the other hand, by using the Komar formula [28,33], we obtain for the total mass of the relativistic disks the expression

$$M_n = \int_0^{2\pi}\int_a^\infty \mu_n e^{\Lambda_n - \Phi_n} r dr d\varphi, \tag{72}$$

which, after using (28) and integrating over φ, reduces to

$$M_n = 8\pi \int_a^\infty \Phi_{n,z} r dr, \tag{73}$$

which, in turn, coincides with the total mass for the corresponding Newtonian disks. Finally, by using (71), it is easy to check that

$$M_n \longrightarrow \infty, \tag{74}$$

for any value of n. That is, all the disks of the family have an infinite mass, a naturally expected result due to the strong divergence of the Newtonian densities at the inner edge.

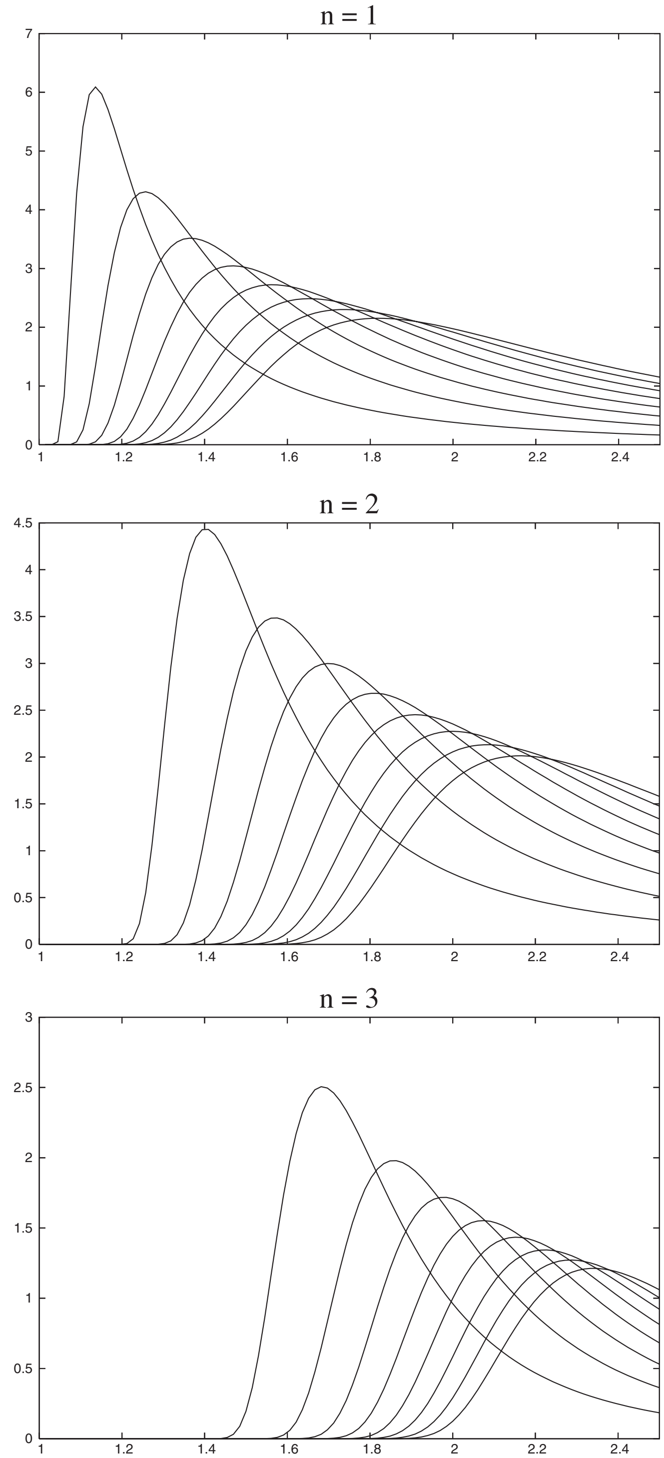

FIG. 1. Surface energy density $\tilde{\epsilon}_n$ as a function of $\tilde{r}$ for the first three disks of the family, with $\tilde{\alpha}_n = 0.5$, 1, 1.5, 2, 2.5, 3, 3.5, and 4. For each value of n, the first curve on the left corresponds to $\tilde{\alpha} = 0.5$, whereas the last curve on the right corresponds to $\tilde{\alpha} = 4$.

Now, since the obtained solutions are asymptotically flat and regular at the symmetry axis, the infinite value of the total mass of the disks is an indication of the presence of a singularity at their inner edge. So, in order to have some insight on the nature of this singularity, we will compute the four Riemann tensor invariants [34]

$$\mathcal{K}_I = R^{abcd}R_{abcd},$$

$$\mathcal{K}_{II} = R^{ab}{}_{kl}R^{klcd}R_{abcd},$$

$$\mathcal{K}_{III} = \frac{\epsilon^{ab}{}_{kl}R^{klcd}R_{abcd}}{\sqrt{-g}},$$

$$\mathcal{K}_{IV} = \frac{\epsilon^{ab}{}_{kl}R^{kl}{}_{mn}R^{mncd}R_{abcd}}{\sqrt{-g}},$$

for all the family of solutions. Here $g = \det g_{ab}$ and ϵ^{abcd} is the Levi-Civita symbol. However, since for any Weyl solution the last two invariants vanish identically, we only need to compute the first two invariants, $\mathcal{K}_I$ and $\mathcal{K}_{II}$.

By using the expressions (55) and (58) for $\Phi_n(x, y)$ and $\Lambda_n(x, y)$, we can cast these two curvature invariants as

$$\mathcal{K}_{In} = -\frac{16\alpha^2 e^{4(\Phi_n - \Lambda_n)} N_{In}(x, y)}{a^{6n+4}(x^2 + y^2)^{12n}}, \tag{75a}$$

$$\mathcal{K}_{IIn} = \frac{48\alpha^3 e^{6(\Phi_n - \Lambda_n)} N_{IIn}(x, y)}{a^{8n+6}(x^2 + y^2)^{16n}}, \tag{75b}$$

where $N_{In}(x, y)$ and $N_{IIn}(x, y)$ are polynomial functions, of highest degree $24n - 6$ and $32n - 9$, respectively, which vanish at the inner edge of the disks,

$$N_{In}(0, 0) = N_{IIn}(0, 0) = 0. \tag{76}$$

We do not write them here explicitly due to their long size.

Moreover, one can check that, in any neighborhood around (0, 0), the difference between $\Phi_n(x, y)$ and $\Lambda_n(x, y)$ behaves as

$$\Phi_n - \Lambda_n \sim -\frac{\alpha^2}{a^{2n}(x^2 + y^2)^{2n}}, \tag{77}$$

so that

$$\lim_{(x,y)\to(0,0)} \frac{e^{4(\Phi_n - \Lambda_n)}}{(x^2 + y^2)^{12n}} = 0, \tag{78a}$$

$$\lim_{(x,y)\to(0,0)} \frac{e^{6(\Phi_n - \Lambda_n)}}{(x^2 + y^2)^{16n}} = 0, \tag{78b}$$

and the limits exist, whatever be the path chosen to approach the point (0, 0).

Then, as a consequence of the above expressions, we have that

$$\lim_{(x,y)\to(0,0)} \mathcal{K}_{In}(x, y) = 0, \tag{79a}$$

$$\lim_{(x,y)\to(0,0)} \mathcal{K}_{IIn}(x, y) = 0, \tag{79b}$$

and thus the Riemann tensor is regular at the inner edge of the disks. However, as it is well known, there are an infinite number of higher invariants constructed from derivatives of the Riemann tensor, so that it is almost certain that some of them will be singular at the inner edge. Therefore, although the Riemann tensor is regular at the inner edge, we cannot ensure that the spacetime will be regular there. Indeed, the presence of this singularity at all the solutions obtained so far describing thin annular disks has been considered by some authors to be tightly connected with the unphysical infinite thinness of the source [35].

V. CONCLUDING REMARKS

We here presented an infinite family of new exact solutions of the Einstein vacuum equations for static and axially symmetric spacetimes. The solutions describe an infinite family of thin dust disks with a central inner edge. Although the strange behavior of the Newtonian potentials may suggest that the disks do not correspond to reasonable astrophysical sources, their energy densities are everywhere positive and well behaved, in such a way that their energy-momentum tensors are in full agreement with all the energy conditions. Moreover, although the total mass of the disks is infinite, the solutions are asymptotically flat and their Riemann tensors are regular everywhere, as is shown by computing the curvature scalars. However, as it was previously pointed out, the infinite value of the total mass of the disks is an indication of the presence of a singularity at their inner edge, a singularity that may be a consequence of considering infinitesimally thin disks as sources.

On the other hand, since all the metric functions of the solutions have been explicitly computed, these are the first fully integrated exact solutions for such thin disk sources. Moreover, the method used here to obtain these explicit solutions may serve as a guideline to find more physical solutions in future works. However, besides their importance as a new family of exact solutions of the Einstein vacuum equations, the main importance of this family of solutions is that it can be easily superposed with the Schwarzschild solution in order to describe binary systems consisting of a thin disk around a central black hole. Indeed, the superposition of the first member of this family with a Schwarzschild black hole has been already performed, and was previously presented in [36]. In a subsequent paper, a detailed analysis of the corresponding superposition for the full family will be presented [37].

Furthermore, the relative simplicity of these solutions when expressed in terms of oblate spheroidal coordinates makes very easy the study of different dynamical aspects, like the motion of particles inside and outside the disks and the stability of the orbits, a study that provides valuable information about the structure and behavior of such gravitational fields. So, although a complete analysis of these dynamical aspects will be presented in another paper, it is worth mentioning that, since $\Phi_{,r} = 0$ at the disk surface, there are not circular orbits on the disk and so a counterrotating interpretation is not possible. However, this situation changes when a black hole is at the center of the disks, as it will be shown in the paper concerning the superposition of this family with the Schwarzschild solution (see [36] for the disk corresponding to the first member of the family).

ACKNOWLEDGMENTS

A. C. Gutiérrez-Piñeres wants to thank the financial support from COLCIENCIAS, Colombia.

[1] A. Celotti, J.C. Miller, and D.W. Sciama, Classical Quantum Gravity **16**, A3 (1999).
[2] M.C. Begelman, Science **300**, 1898 (2003).
[3] O. Semerák, *Gravitation: Following the Prague Inspiration (To Celebrate the 60th Birthday of Jiri Bic ák)*, edited by O. Semerák, J. Podolský, and M. Žofka (World Scientific, Singapore, 2002), p. 111.
[4] V. Karas, J.-M. Hure, and O. Semerák, Classical Quantum Gravity **21**, R1 (2004).
[5] J.P.S. Lemos and P.S. Letelier, Classical Quantum Gravity **10**, L75 (1993).
[6] J.P.S. Lemos and P.S. Letelier, Phys. Rev. D **49**, 5135 (1994).
[7] J. P. S. Lemos and P. S. Letelier, Int. J. Mod. Phys. D **5**, 53 (1996).
[8] T. Morgan and L. Morgan, Phys. Rev. **183**, 1097 (1969).
[9] O. Semerák, T. Zellerin, and M. Žáček, Mon. Not. R. Astron. Soc. **308**, 691 (1999); **322**, 207(E) (2001).
[10] O. Semerák, M. Žáček, and T. Zellerin, Mon. Not. R. Astron. Soc. **308**, 705 (1999).
[11] O. Semerák and M. Žáček, Publ. Astron. Soc. Jpn. **52**, 1067 (2000).
[12] O. Semerák and M. Žáček, Classical Quantum Gravity **17**, 1613 (2000).
[13] O. Semerák, Czech. J. Phys. **52**, 11 (2002).
[14] M. Žáček and O. Semerák, Czech. J. Phys. **52**, 19 (2002).
[15] O. Semerák, Classical Quantum Gravity **20**, 1613 (2003).
[16] O. Semerák, Classical Quantum Gravity **21**, 2203 (2004).
[17] C. Klein, Classical Quantum Gravity **14**, 2267 (1997).
[18] T. Zellerin and O. Semerák, Classical Quantum Gravity **17**, 5103 (2000).
[19] O. Semerák, Classical Quantum Gravity **19**, 3829 (2002).
[20] C. Klein, Phys. Rev. D **68**, 027501 (2003).
[21] C. Klein and O. Richter, *Ernst Equation and Riemann Surfaces: Analytical and Numerical Methods*, Lect. Notes Phys. Vol. 685 (Springer, Berlin, 2005).
[22] L. Morgan and T. Morgan, Phys. Rev. D **2**, 2756 (1970).
[23] A. Papapetrou and A. Hamouni, Ann. Inst. Henri Poincaré **9**, 179 (1968).
[24] A. Lichnerowicz and C. R. Acad, Science **273**, 528 (1971).
[25] A. H. Taub, J. Math. Phys. (N.Y.) **21**, 1423 (1980).
[26] E. Israel, Nuovo Cimento B **44**, 1 (1966).
[27] E. Israel, Nuovo Cimento B **48**, 463 (1967).
[28] E. Poisson, *A Relativist's Toolkit: The Mathematics of Black-Hole Mechanics* (Cambridge University Press, Cambridge, England, 2004).
[29] H. Stephani, D. Kramer, M. MacCallum, C. Hoenselaers, and E. Herlt, *Exact Solutions of Einstein's Field Equations* (Cambridge University Press, Cambridge, England, 2003).
[30] G. A. González and O. A. Espitia, Phys. Rev. D **68**, 104028 (2003).
[31] H. Bateman, *Partial Differential Equations* (Dover, New York, 1944).
[32] S.W. Hawking and G.F.R. Ellis, *The Large Scale Structure of Space-Time* (Cambridge University Press, Cambridge, England, 1973).
[33] R.M. Wald, *General Relativity* (University of Chicago, Chicago, 1984).
[34] S. Weinberg, *Gravitation and Cosmology: Principles and Applications of the General Theory of Relativity* (John Wiley & Sons, New York, 1972).
[35] J. Šácha and O.O. Semerák, Czech. J. Phys. **55**, 139 (2005).
[36] G.A. González and A.C. Gutiérrez-Piñeres, arXiv: 0811.3002v1.
[37] G.A. González and A.C. Gutiérrez-Piñeres, Relativistic static thin disks around a central black hole: An infinite family of new exact solutions (unpublished).